# **Effects of Cell Phone Radiation on the Head**

BEE 4530
Computer-Aided Engineering: Applications to Biomedical Processes

Group 3
Angela Cai
Youjin Cho
Mytien Nguyen
Praveen Polamraju

# Table of Contents

## I. Executive Summary

The brain is sensitive to small changes in temperature. Temperature increases may affect enzyme function, leading to possible negative biological effects. Living tissues are dielectric materials, which are subjected to dielectric heating by radiation.

A common source of radiation is the cell phone. People often hold cell phones next to their ears, which may exacerbate the effects of radiation, and therein, temperature change. The rate at which tissue absorbs heat from radiation is called the specific absorption rate (SAR). Through observations of SAR values, the thermal effect of the electromagnetic wave heating of superficial tissue within the brain can be quantified.

The goal of this project is to model heating of tissue layers in the brain due to cell phone radiation exposure in order to evaluate implications of cell phone usage on brain function. Cranial temperature profiles were studied with varying cell phone distances from the ear, usage durations, and radiation intensities.

Cell phone radiation in a model head was simulated in COMSOL Multiphysics 4.3b using governing equations for electromagnetic waves and temperature. Maxwell's equation for electromagnetic waves was used to determine the electric field and the SAR that would determine heat generation terms. The three-dimensional heat equation was then used to determine the increase in temperature within the brain after a specific period of time. Three dimensions were necessary since there is no symmetry within the head in the presence of a cell phone. To accurately simulate thermoregulatory processes in the head, metabolic heat generation from these tissues and convective blood flow were included in the heat equation.

Values for thermal conductivity, skull dimensions, metabolic heat generation, emissivity, radiofrequency, and power dissipation rate were found in relevant literature. In addition, we compared increases in temperature in the brain model with values found in literature to give us an approximation. The results indicate that after two hours of cell phone usage, the maximum increase in brain temperature was slightly greater than 0.2°C in an adult.

These results show that there is a minimal effect on cranial temperature by cell phone radiation, even after a significant amount of cell phone usage. The head's thermoregulatory processes of insulating layers and convective blood flow seem to successfully maintain brain temperature within 0.2°C. Thus, brain function is not severely impacted by the thermal effect of cell phone radiation. However, this model may help develop more accurate guidelines for appropriate cell phone usage.

## II. INTRODUCTION: CELL PHONE RADIATION AND OUR HEALTH

The use of mobile phones began in the 1980's and has rapidly increased since then [1]. In the ten years between 2000 and 2010, cell phone use has increased threefold [1]. In 2008, about 87% of the U.S. population was subscribed to cell phones plans [2]. As mobile phone usage becomes more advanced and common worldwide, the effects of radiation caused by these devices are becoming a bigger concern. Cell phone radiation has been linked to brain cancer, salivary gland tumors, behavioral problems, and migraines. These risks have been shown to be higher in people who have used cell phones for at least ten years [1]. However, studies on brain cancer cast doubt on these results since it is difficult to accurately assess risk factors in humans [3].

Specifically, radiation emitted by cell phones is in the form of non-ionizing radiofrequency energy [4]. This electromagnetic radiation has both direct and indirect effects on the body. The heat caused by electromagnetic waves is a direct effect that can damage tissues and organs. This heat is measured by the Specific Absorption Rate, or SAR. The indirect effects caused by radiation have not been shown to have any significant effects on human health [4]. Because of the increasing necessity of mobile phones in our daily lives, it is very important to determine the health effects of cell phone radiation under various conditions.

Previous projects have studied the effects of cell phone radiation on body temperature. A study published by Wainwright [5], using an average phone output of 2 Watts, concluded that the maximum temperature increase would be around 1°C. Other studies have been done on the effects of radiation on cancer risk and various brain sizes (children and adults). The study conducted by Wessapan and Rattanadecho [6] confirms that temperature effects are significantly different in organs of children, compared to adults. While adults have a greater increase in skin temperature, children have a greater increase in brain temperature [6]. In addition, Wiart *et al.* [7] concluded that children's heads would absorb twice as much radiation as adult heads.

On the other hand, radiation emitted by mobile phones may actually be useful instead of harmful. Some studies have reported beneficial effects caused by cell phone radiation. A study done on university students concluded that 10 minute exposures to cell phone electromagnetic fields led to decreased reaction times [8]. This is advantageous in dangerous situations. Several other studies have examined cell phone radiation effects in relation to Alzheimer's disease. These studies have found that cell phone radiation may actually improve cognitive functions and may reduce plaque deposition in the brain, a characteristic of Alzheimer's disease [9]. Further studies could lead to breakthroughs in the treatment of neurodegenerative diseases, such as Alzheimer's. However, very few studies have been done on the advantages of mobile phone radiation. Because of the changing types of phones, frequencies, and durations of cell phone use, studies relating cancer risk to radiation from mobile phones have not been consistent. Thus, the biological effects of mobile phone radiation are still unclear. We hope this project will help increase our understanding of the effects of mobile phone radiation.

## III. Problem Statement and Proposed Solution

Our project aims to evaluate the effect of radiation exposure on tissue heating by performing 2D and 3D modeling of radiation to the head in COMSOL Multiphysics 4.3b. The effects of cell phone radiation on tissue temperature have been modeled in the past, demonstrating a 0.2°C increase in the brain. Our model will expand on current models and simulate cell phone radiation in the brain with varying voltages and thermal properties. These modifications account for personal cell phone usage preferences and provide more realistic results of tissue heating by cell phone radiation.

## IV. Design Objectives

Our goal is to analyze how cell phone electromagnetic wave radiation affects the brain. We plan to use computational modeling to study the following:

1. Develop a model in COMSOL to analyze the temperature profile in the brain and ear.
2. Utilize both 2D and 3D models to evaluate how the different tissue layers (skin, skull, brain layers) minimize heat transfer of electromagnetic waves to the brain.
3. Determine how different voltages and thermal properties affect the temperature profile due to cell phone radiation.

## V. Governing Equations

Electromagnetic waves from the cell phone travel through air and penetrate tissue layers inside the head. The amount of electromagnetic waves absorbed within each tissue layer is dependent on tissue properties. The absorbed electromagnetic radiation is, in turn, a source of heat generation, and the corresponding heat term can be calculated using Equation 2. As we can see, the more electrically conductive the tissue layer, the greater the heat generated by a given electric field magnitude. This electromagnetic heat source, in turn, increases the temperature at a given position inside the tissue layer.

In our model, electromagnetic and thermal computations were coupled by first determining the electric field profile within the tissue layers. This electric field profile can then be used to determine the temperature increase as it varies with distance from the surface. We define our temperature and electromagnetic governing equations as below:

**Temperature**: thermal profile within the brain and outer layers (skin, fat, and skull) due to metabolism, electromagnetic absorption, and blood flow.

$$\rho_{tissue} C_{tissue} \frac{\partial T}{\partial t} = \nabla(k \nabla T) + \rho_b C_b \omega_b (T_b - T) + Q_{EM} + Q_{metabolism}$$ [**Equation 1**]

$$Q_{EM} = \frac{1}{2} \sigma_{tissue} |E|^2$$ [**Equation 2**]

$Q_{metabolism}$ is the heat generated from metabolism in watts per volume, and $Q_{EM}$ is the heat generated from the electromagnetic radiation.

**Electromagnetic radiation**: wave propagation of the electric field, obtained from Maxwell's Equations without a magnetic field ($\nabla B = 0$):

$$\nabla \frac{1}{\pi_r} \nabla E - k_0^2 \varepsilon_r E = 0$$ [**Equation 3**]

COMSOL Multiphysics 4.3b was used to solve these two governing equations with the appropriate boundary conditions outlined below.

## VI. Schematic of our 2D and 3D Models

To model electromagnetic radiation to the head, we will compute the temperature change in the head in both 2D (Figure 1) and 3D (Figure 2). A 2D model allows us to visualize heating inside the different layers of the head, and a 3D model provides more realistic computation of electromagnetic wave propagation into the head layers. The schematics of our 2D and 3D models are defined below. For 3D model, instead of having different layers within the head model, we used "sar_in_human_head_interp.txt" file which contains interpolated values of the head with 109 slices of a magnetic-resonance image (MRI) [10].

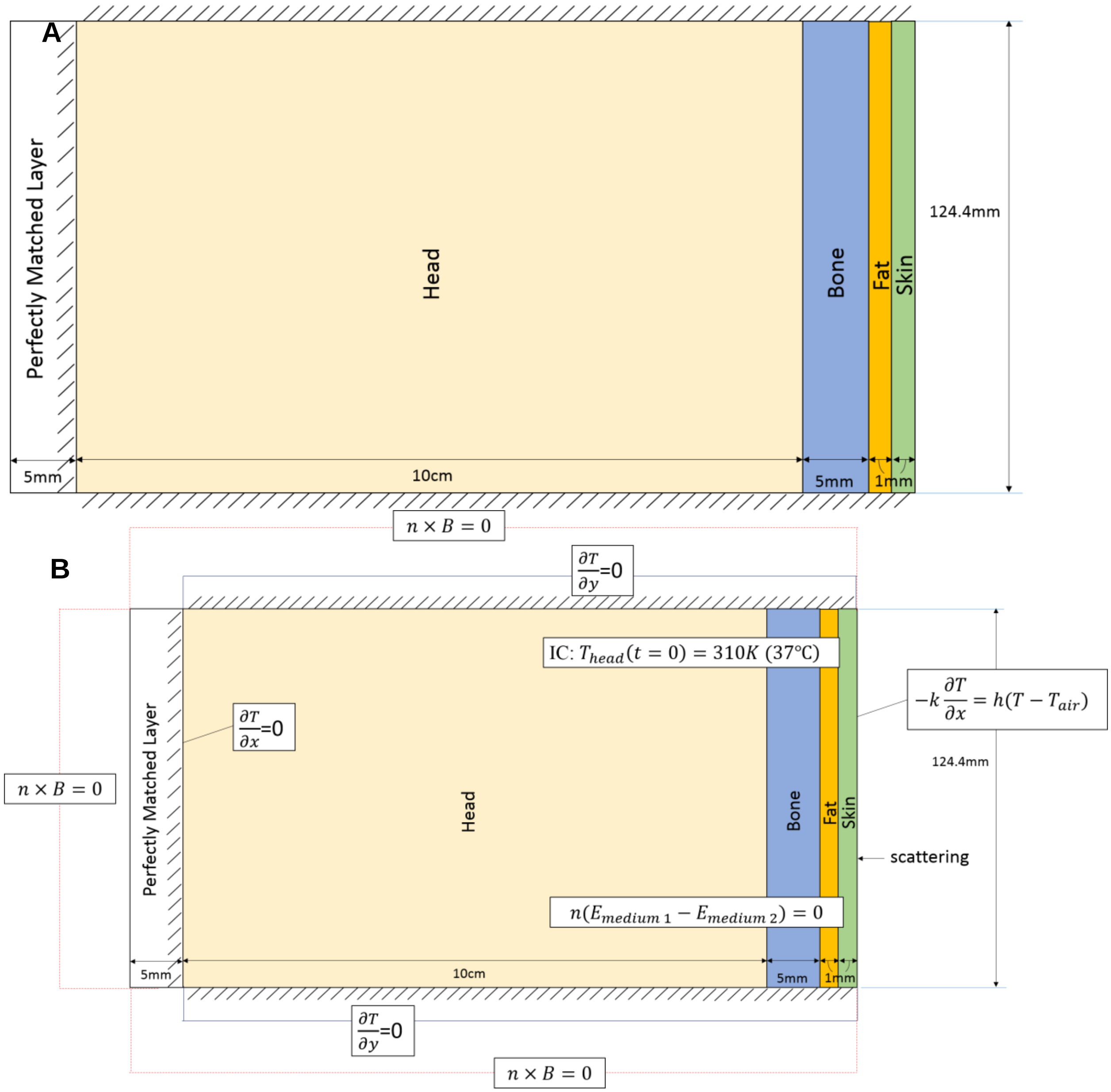


**Figure 1**: Two-dimensional model of head layers. (**A**) There exists a layer of air next to the head (skin layer) and cell phone boundaries (scattering boundary), resulting in a convective heat transfer term (Equation 5). The cell phone domain is modeled as a boundary condition in COMSOL. (**B**) Thermal and electromagnetic boundary conditions, as well as initial conditions, are as shown.

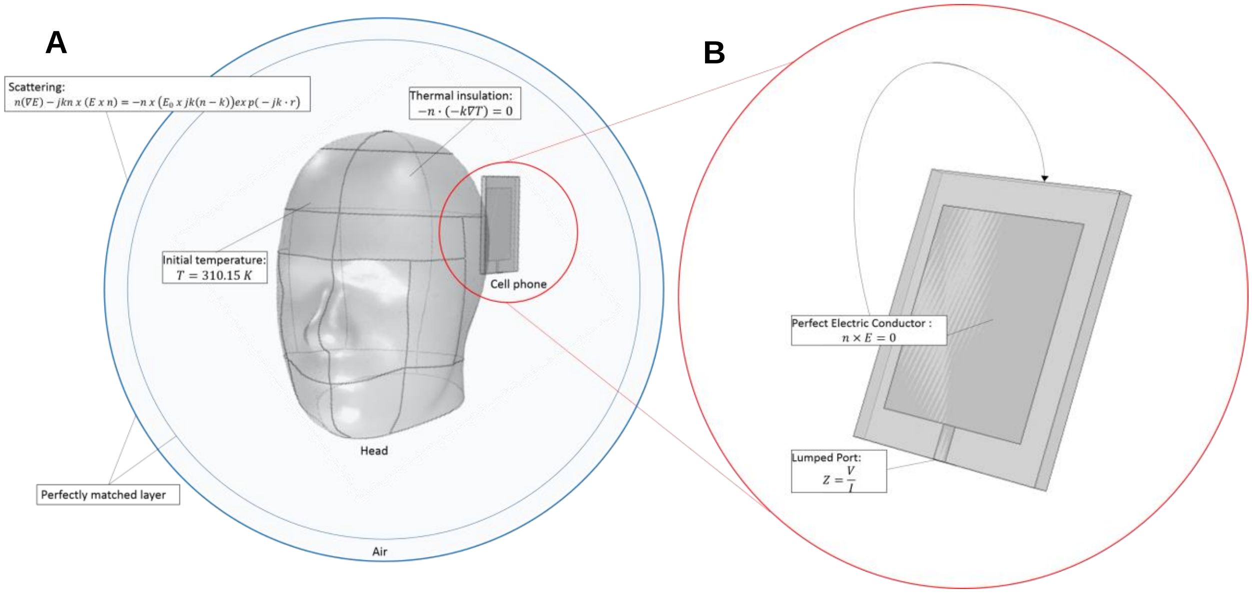


**Figure 2**: Three-dimensional model of: (**A**) the head, cell phone, and spherical air domain. (**B**) A close up of the cell phone domain, with the cell phone modeled as a rectangular lumped port at the bottom.

## VII. Boundary and Initial Conditions For Heat Transfer and Electromagnetic Equations

The following thermal and electromagnetic conditions were inputted into COMSOL to solve the coupled temperature and electromagnetic governing equations:

### Thermal boundary conditions:

In previous studies [6], electromagnetic radiation did not penetrate further than half the head's width. Therefore, we can assume semi-infinite geometry into the brain. In 2D, there is no heat flux along the inner boundary of the brain layer and the top and bottom layers not in contact with the cell phone (Figure 1). In 3D, the outer surface of the brain is thermally insulated (Figure 2).

$$\frac{\partial T}{\partial x} = 0 \; and \; \frac{\partial T}{\partial y} = 0$$ [**Equation 4**]

In 2D, the left boundary of the skin layer is exposed to the air, so we apply the convective boundary condition.

$$-k\frac{\partial T}{\partial x} = h(T - T_{air})$$ [**Equation 5**]

**Electromagnetic boundary conditions:**

We make use of a perfectly matched layer boundary in both the 2D (left boundary) and 3D (air) models [10]. This boundary allows electromagnetic waves to be "absorbed" by the boundary and prevents reflection of waves back to tissue layers, which is useful for open boundaries (i.e. air).

For simplicity of computation, we assume that electrical property differences between the tissue layers do not affect electromagnetic wave propagation. This allows us to apply continuity boundary conditions along the interfaces between different media (i.e. between skin and fat, fat and bone, and bone and brain) in both 2D and 3D:

$$n(E_{medium\ 1} - E_{medium\ 2}) = 0$$ [**Equation 6**]

Along the top, bottom, and left surfaces of the 2D model, we use the perfect magnetic conductor boundary condition. We assume that these surfaces have high surface impedance: electric fields and tangential magnetic fields cannot pass through these boundaries, resulting in a zero electric field magnitude, a characteristic of conductors. The perfect magnetic conductor boundary condition is analogous to the no flux boundary condition in heat transfer.

$$n \times B = 0$$ [**Equation 7**]

Along the outside surface of the skin exposed to the cell phone in 2D, we have a scattering boundary condition for the source term from the cell phone ($E_0$=40.3 V/m), where waves orthogonal to the surface completely escape the tissue as if the surface is transparent, while all other waves are reflected back into the tissue. In 3D, this is only applied to the air spherical domain.

$$n(\nabla E) - jkn\ x\ (E\ x\ n) = -n\ x\ \left(E_0\ x\ jk(n-k)\right)exp(-jk \cdot r)$$ [**Equation 8**]

where $n$ is the normal vector, and $j = \sqrt{-1}$

In 3D, the cell phone is modeled with perfect electrical conductor boundary conditions on the front and back surfaces (Figure 2):

$$n \times E = 0$$ [**Equation 9**]

The antenna is modeled as a lumped port on the bottom rectangle of the cell phone domain:

$$Z_{in} = \frac{V_1}{I_1}$$ [**Equation 10**]

**Initial condition:**

In our transient model, we assume that the head is at biological functional temperature at the start (time=0s):

$$T_{head}(t = 0) = 310.15K\ (\sim 37°C)$$ [**Equation 11**]

## VIII. Results and Discussion of our Computational Models

### 2D Model:

After creating our 2D model, we determined temperature increase after one hour, electric field strength distribution throughout the head, and the heat source term due to electromagnetic radiation. The electric field and heat source term do not vary with time because we solve the electromagnetic wave equation using a frequency domain in COMSOL, independent of time.

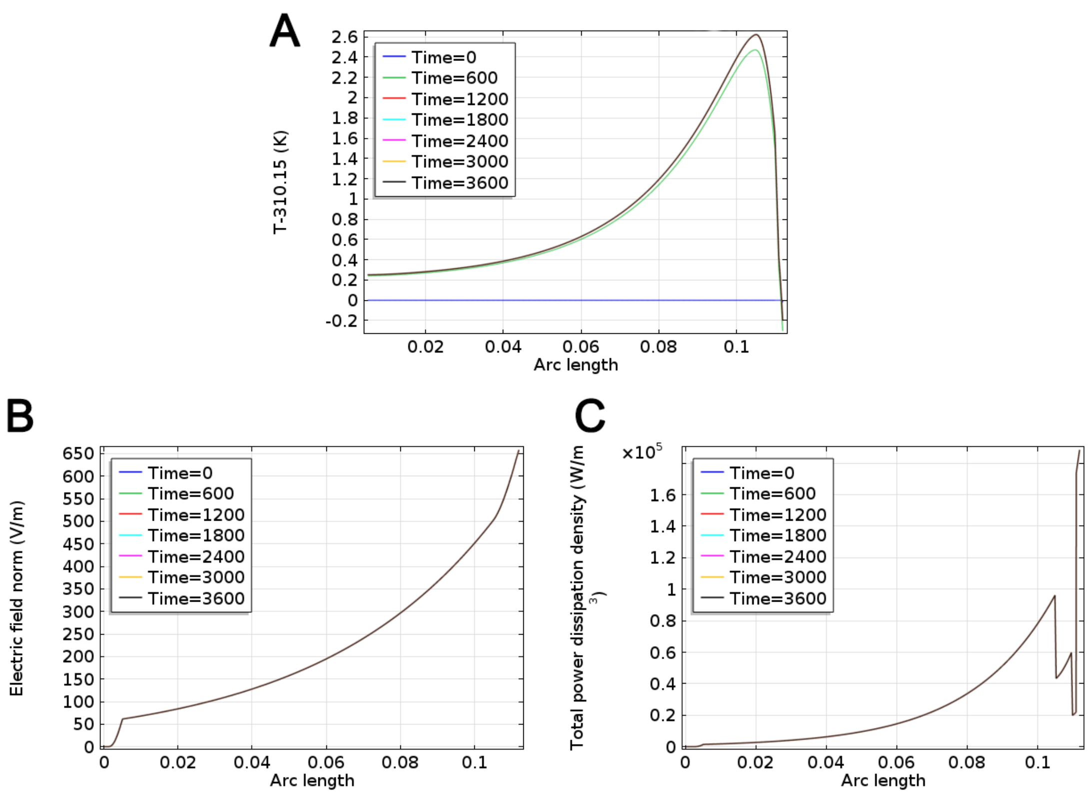


**Figure 3**: 2D temperature profiles of the head: (**A**) temperature increase over time (in seconds) and position. There is a 2.6°C difference between the maximum temperature and the initial (and arterial) temperatures. (**B**) Electric field norm over time and position. There is no significant difference in electric field norm over time. (**C**) Power dissipation in the head over time and position. There is no significant difference in power dissipation due to electric field over time.

In our simplified 2D model, we observed a temperature increase of 2.6°C between the maximum temperature and initial temperature in a region of the brain when convection was ignored on the right boundary (flux=0) (Figure 3). In addition, we found that temperature stopped changing with time after 1800 s (Figure 3). In reality, it would be more accurate to create a domain for the cell phone itself when solving the electromagnetic wave equation. Perfect magnetic conductor boundaries on the left, right, and top boundaries of the cell phone and a power source boundary on the bottom could be applied to simulate more realistic parameters [6]. However, our model was able to capture the significant physics by successfully incorporating electromagnetic heating as a source term in the heat equation, contributing to an increase in temperature observed in Figure 3.

**3D Model:**

In our 3D model, we found the maximum temperature increase in our model after one hour, temperature variation near the surface of the head over time, and the SAR distribution in the head. Similarly to our 2D model, the SAR distribution does not vary with time because we solved the electromagnetic wave equation using the frequency domain in COMSOL.

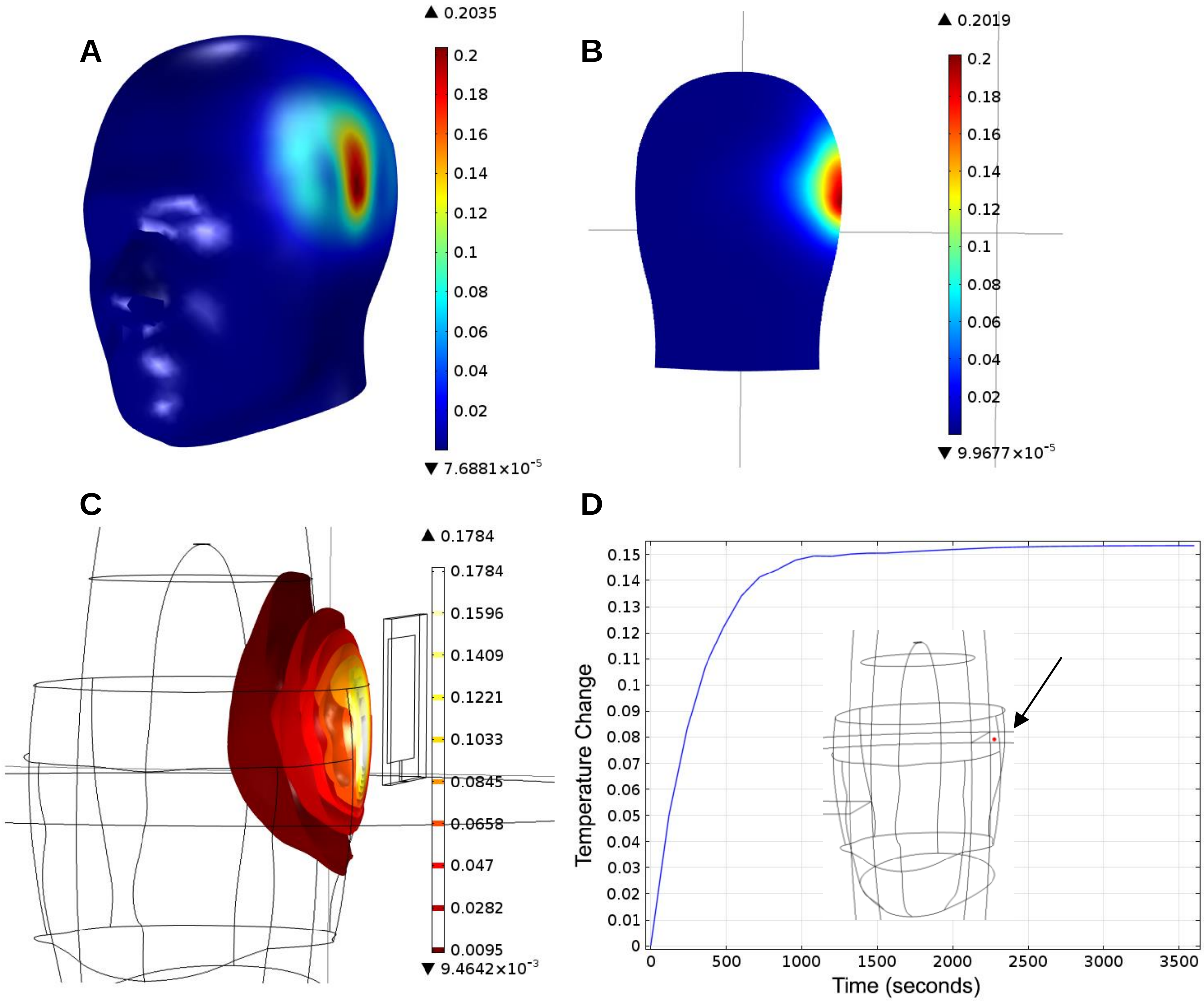


**Figure 4**: 3D temperature profiles of the head: (**A**) Temperature profile of the whole head, and (**B**) of a frontal plane slice, after 60 minutes of cell phone exposure. (**C**) Isothermal contours within the head after 60 minutes of cell phone exposure. (**D**) Time-dependent temperature profile at a point right inside the head (as indicated by the red dot) for 60 minutes of cell phone exposure. At the surface of the head, there is a 0.2°C difference between the maximum temperature and the initial (and arterial) temperatures, with temperature reaching steady state after 2500 seconds (approximately 42 minutes).

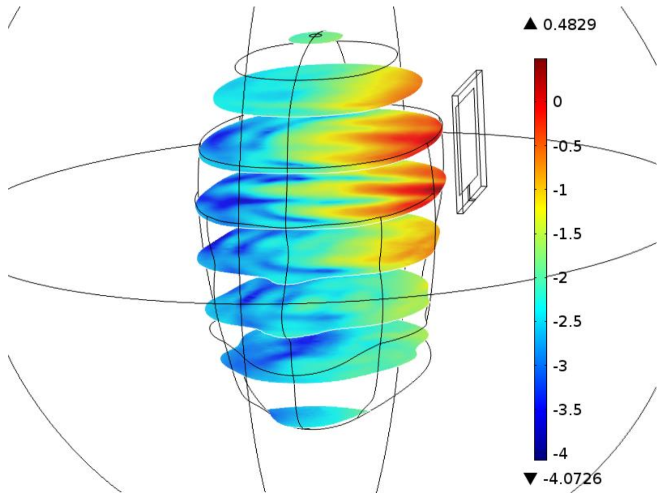


**Figure 5**: Log scale of the local SAR value in the brain. In concurrence with the temperature profile, the SAR absorption is greatest closer to the cell phone ($SAR_{max}$ = 1W/kg).

In our 3D model, we observed a temperature increase of 0.2°C, one magnitude less than that found in our 2D model (Figure 4). The maximum temperature increase occurred near the surface of the head, with the greatest SAR associated with it (Figures 4, 5). In addition, the temperature stops changing with time after about 2500 s (Figure 4). This is due to the computational differences between 2D and 3D modeling and the varying far right boundary condition choices. In addition, our 3D model only simulates varying electrical properties of the brain layers, not thermal properties. In the 2D model, a simplified scattering boundary condition was applied as the far right boundary condition with a specified electric field magnitude.

**Sensitivity Analysis:**

We performed sensitivity analysis on the applied electric field, ambient air temperature, and the heat transfer coefficient in our 2D model. Predictably, temperature change inside the head increased with increasing applied electric field magnitude (Figure 6A). Temperature change is also linearly dependent on the heat transfer coefficient (for example, wind speed) and air temperature (Figure 6B). At a given heat transfer coefficient, temperature change inside the head increased with increasing air temperature. This implies that a temperature increase in the brain is more significant in the summer than in the winter.

In addition, with changing heat transfer coefficients, there is a positive linear relationship with temperature change when air temperature is above body temperature and a negative linear relationship when air temperature is below body temperature. Heat transfer coefficient simply enhances the heat removal (when $T_0 < 37$°C) or heat absorption (when $T_0 > 37$°C) effects of the ambient temperature. For small changes in heat transfer coefficient ($\pm$10%), the temperature increase would change by about 0.2°C.

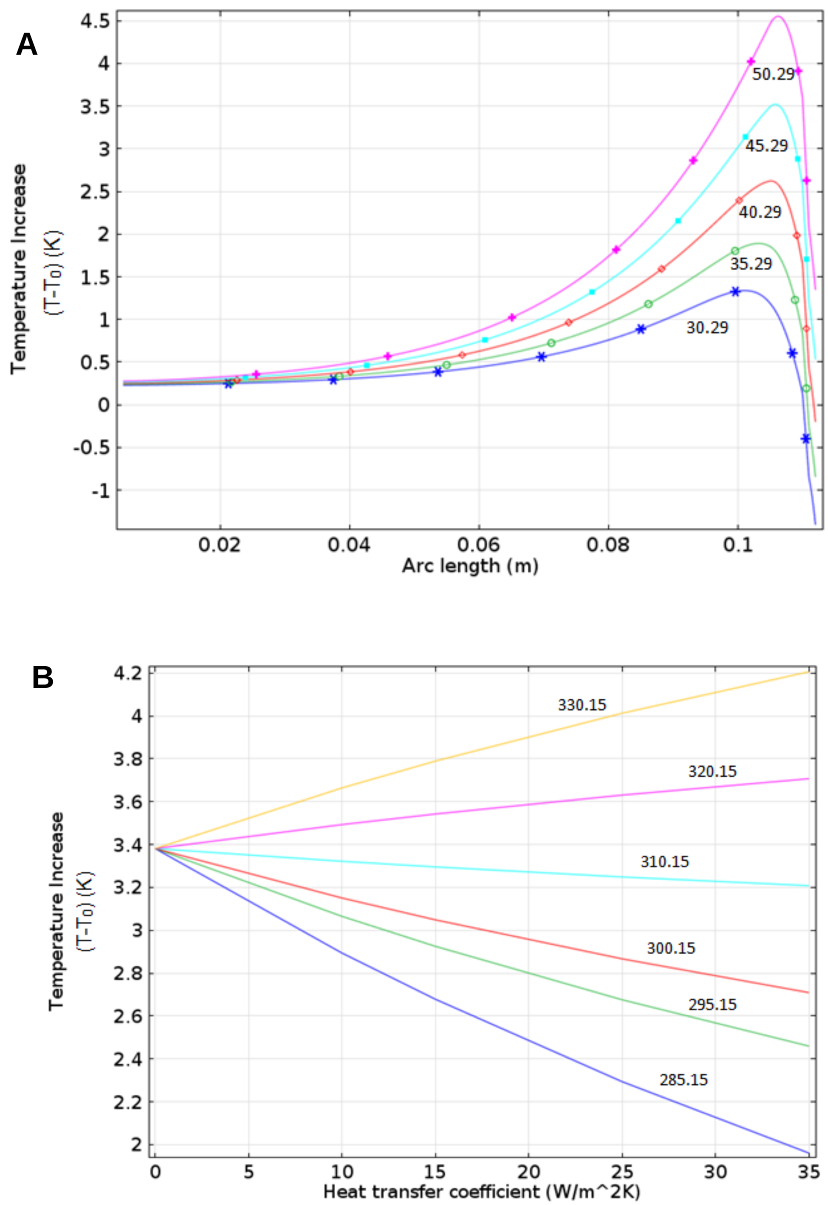


**Figure 6**: Temperature increase from normal body temperature (37°C) as a function of (**A**) electric field input and (**B**) heat transfer coefficient and ambient temperature $T_{air}$, after 60 minutes of cell phone radiation exposure in the 2D model. The ambient temperature is represented by the various lines. For ambient temperatures greater than initial temperatures, an increase of heat transfer coefficient causes a higher temperature increase. However, if ambient temperatures are lower than initial temperature, then an increase of heat transfer coefficient causes a higher temperature decrease.

Sensitivity analysis for our 3D model was completed with varying electric fields, initial temperatures, and thermal conductivities. Near the center of the head, we observed the greatest change in temperature due to varying electric fields (Figure 7A). At the surface of the head, the effect of increasing electric fields was negligible. The effect of varying initial temperature on temperature across the head after 60 minutes was also negligible (Figure 7B). Thus, small changes in initial temperature do not affect overall results in our 3D model.

Temperature sensitivity to thermal properties was analyzed by varying the thermal conductivities from 0.22 W/mK to 0.5 W/mK. These values were selected from the range of thermal conductivities for the different tissue layers (skin, bone, brain, and fat). The resulting temperature effect of thermal conductivity is significant with a difference of approximately 0.025 K between the minimum and maximum values. This indicates that the radiation effect in the head is sensitive to thermal properties, and we must ensure that our values are as accurate as possible.

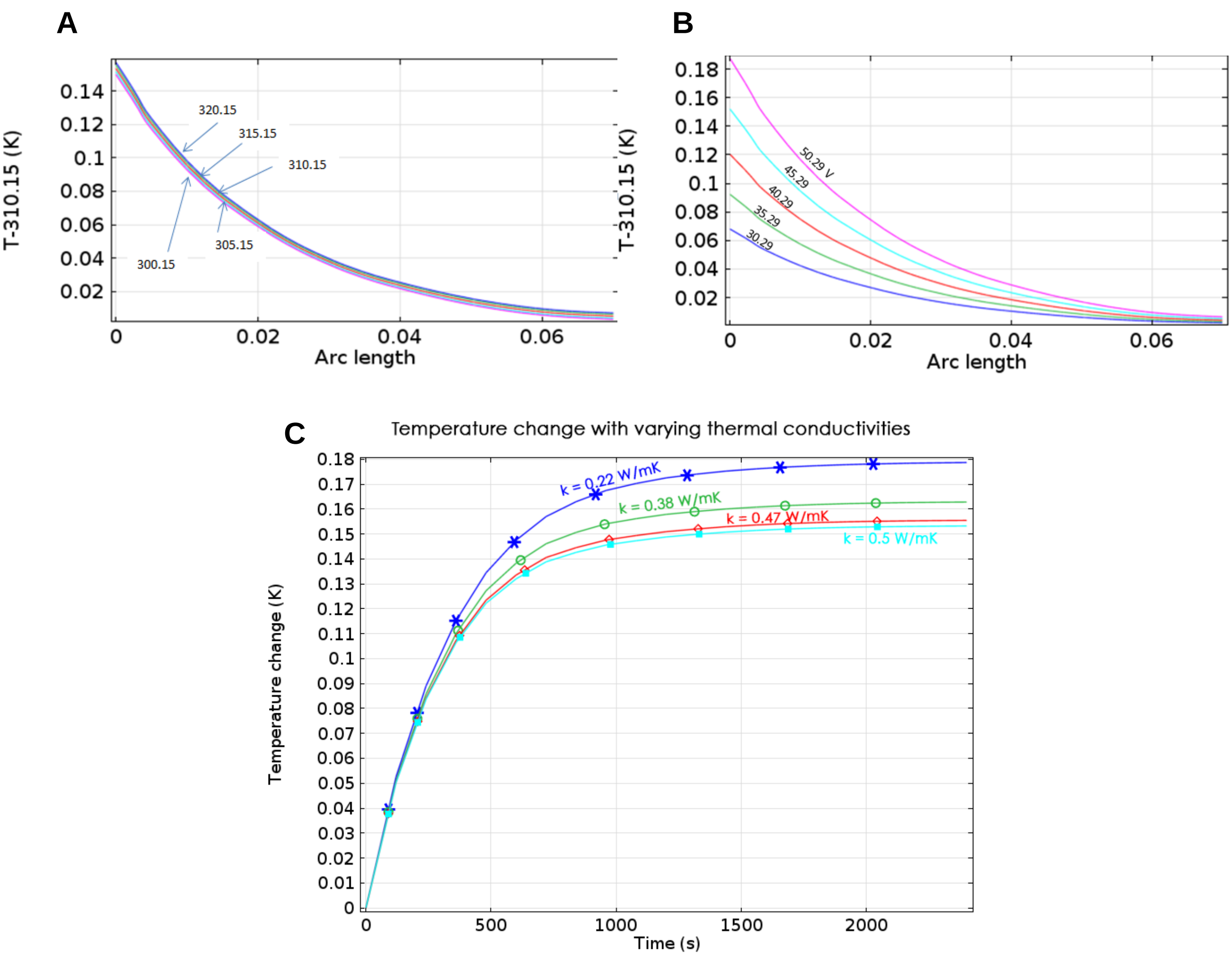


**Figure 7:** Temperature increase from normal body temperature (37°C) as a function of position with varying (**A**) electric field in the 3D model and (**B**) initial temperature after 60 minutes. (**C**) Temperature change at different thermal conductivity values in the brain after 30 minutes.

## Accuracy Check:

In order to validate the results of our 2D model, we compared our temperature increase in the head with that of Dlouhý in literature [4]. The temperature change (calculated as the difference between maximum and initial temperature) for our 2D model was about 2.8°C after 6 minutes (Figure 3A). Compared to our values, the maximum temperature increase in the Dlouhý model after 6 minutes were significantly less: 0.0085 °C and 0.0019°C temperature increases for cell phone frequencies of 900 MHz and 1800 MHz, respectively. This large difference in the temperature change may be due to the fact that our SAR values were significantly different from each other. Through an external source, "Czech cod no. 480/2000", they assumed that for each cell phone user, the SAR value must not be higher than 0.08 $Wkg^{-1}$. Based on this assumption, they used modified tissue property values. By doing so, they were able to obtain a SAR value of 0.0516 $Wkg^{-1}$.

However, compared to their value, the value that we used was 1.25 W/kg for the iPhone 5 (the current most popular model) [11]. Due to this difference, there was a significant increase in the calculated electric field value, resulting in the greater increase in temperature for our 2D model. In addition, the 3D model with fewer assumptions may be a more accurate model for data analysis on the effect of cell phone radiation on temperature increase in the head. Comparing the boundary conditions between 2D and 3D model, the 3D model contains scattering boundary condition on the outer layer of the air. As a result, for 3D model only a portion of the electromagnetic waves reach the head whereas for 2D model all the electromagnetic waves radiated from the cell phone source reaches the head.

To validate our results for the 3D model, we compared our maximum temperature increase in the head with that of Wessapan and Rattanadecho in literature [6]. The maximum temperature increase in our 3D model from the initial temperature was about 0.2°C after an hour. After 30 minutes, Wessapan and Rattandecho found a maximum temperature increase of 0.118°C. Based on our 3D model of temperature versus time results (Figure 4D), the head temperature did not reach a steady state value after 30 minutes, with a temperature increase of approximately 0.15°C at the 30 minute mark. The slight difference between the temperature increase found in the literature and our model may be due to our lack of thermal property interpolation within the head layers. In addition, we compared our SAR profiles with those in literature and both reported a maximum SAR increase of approximately 1 W/kg [6] (Figure 5).

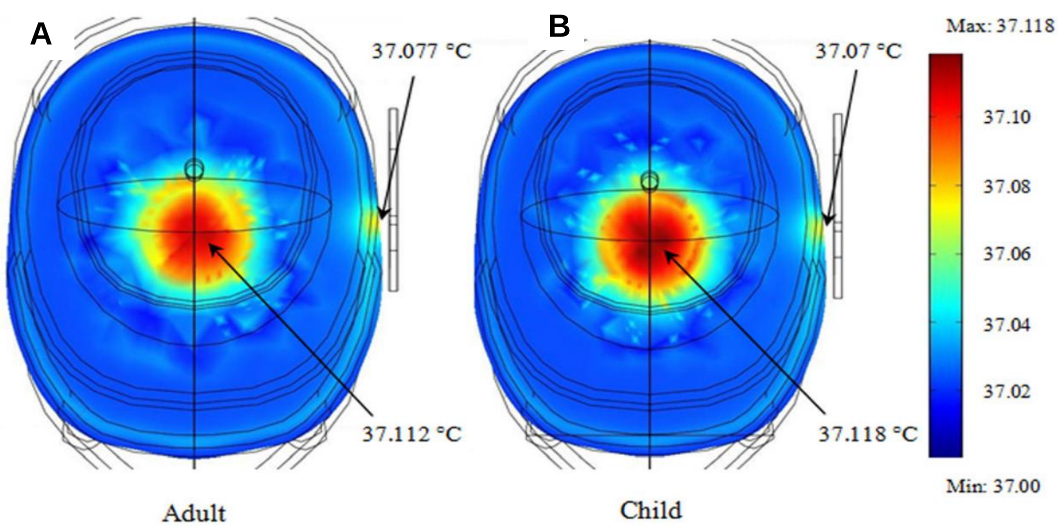


**Figure 8:** (**A**) Temperature profile of the head after 30 minutes by Wessapan and Rattanadecho [6]. (**B**) SAR measured in the head after 30 minutes by Wessapan and Rattanadecho [2]. Our 2D results reported a maximum temperature increase in the head of greater than 2°C. In our model, we created a constant electric field boundary at the end of the head, which most likely led to the higher increase in temperature than predicted with our 3D model.

## IX. CONCLUSION AND DESIGN RECOMMENDATIONS

We implemented our study in 2D and 3D to model the thermal effect of cell phone radiation on the head. While our simplified 2D model reduced computation time significantly, it generated a maximum temperature increase of 2.6°C while our 3D model generated a maximum temperature increase of 0.2°C. This might be due to the relative higher electromagnetic wave magnitude in 2D from the scattering boundary condition used. However, our 3D model suggests that there is a minimal temperature increase in the brain due to cell phone radiation. In sensitivity analysis, we showed that temperature increase depends on both voltage source and thermal conductivity. A higher voltage source would generate a greater temperature increase. This shows that it is imperative to keep electric field below specific thresholds to prevent brain damage.

However, a higher thermal conductivity would result in a lower temperature. This unexpected correlation is due to the effect of thermal diffusivity on radiation: a higher thermal diffusivity (from a higher thermal conductivity) may increase heat transfer between heated and unheated regions, minimizing the effect of radiation on tissues.

### Design Recommendations:

For an average adult, a maximum of approximately 50 V in a cell phone antenna should be applied to minimize temperature increase in the brain. However, additional side effects need to be considered when using this voltage. As our study indicates, temperature change reaches a steady state after 42 minutes of radiation exposure, but a lower exposure time is always advisable.

### Limitations and Future Works:

There are several assumptions inherent in our models that may limit their applicability. For example, we assumed that electromagnetic waves are continuous between tissue layers throughout the head. However, since tissue layers have different electromagnetic properties, the nature of electromagnetic wave propagation may be affected by these differences. More realistic models may show a slight difference in temperature distribution within the head.

Future studies in this field could look at the effect of varying head dimensions and properties on the thermal effects of radiation. This study would reflect variations in a diverse population, from adults to children, and to model tissue properties changes with age. In addition, the location of the cell phone also remained constant in our model. Distance from cell phone to the head differs on an individual basis, future studies could also vary the position of the cell phone from the surface of the head.

## X. APPENDIX A

**A. Table A: Constant Input Parameters.** These values are assumed to be constant in the modeling process.

| Input Parameter | Definition | Value | Units | Source |
|---|---|---|---|---|
| $\rho_{brain}$ | Brain tissue layer density | 1030 | $\frac{\mathrm{kg}}{\mathrm{m}^3}$ | [5] |
| $\rho_{bone}$ | Bone (skull) layer density | 1850 | $\frac{\mathrm{kg}}{\mathrm{m}^3}$ | [5] |
| $\rho_{fat}$ | Fat layer density | 1100 | $\frac{\mathrm{kg}}{\mathrm{m}^3}$ | [5] |
| $\rho_{skin}$ | Skin layer density | 1100 | $\frac{\mathrm{kg}}{\mathrm{m}^3}$ | [5] |
| $\rho_b$ | Blood density | 1060 | $\frac{\mathrm{kg}}{\mathrm{m}^3}$ | [5] |
| $C_{brain}$ | Brain tissue layer specific heat capacity | 3680 | $\frac{\mathrm{J}}{\mathrm{kgK}}$ | [5] |
| $C_{bone}$ | Bone (skull) layer specific heat capacity | 1300 | $\frac{\mathrm{J}}{\mathrm{kgK}}$ | [5] |
| $C_{fat}$ | Fat layer specific heat capacity | 2325 | $\frac{\mathrm{J}}{\mathrm{kgK}}$ | [5] |
| $C_{skin}$ | Skin layer specific heat capacity | 3430 | $\frac{\mathrm{J}}{\mathrm{kgK}}$ | [5] |
| $C_b$ | Blood specific heat capacity | 3840 | $\frac{\mathrm{J}}{\mathrm{kgK}}$ | [5] |
| $k_{brain}$ | Brain tissue layer thermal conductivity | 0.5395 | $\frac{\mathrm{W}}{\mathrm{mK}}$ | [5] |
| $k_{bone}$ | Bone (skull) layer thermal conductivity | 0.4345 | $\frac{\mathrm{W}}{\mathrm{mK}}$ | [5] |
| $k_{fat}$ | Fat layer thermal conductivity | 0.223 | $\frac{\mathrm{W}}{\mathrm{mK}}$ | [5] |
| $k_{skin}$ | Skin layer thermal conductivity | 0.266 | $\frac{\mathrm{W}}{\mathrm{mK}}$ | [5] |
| $h$ | Heat transfer coefficient in air | 25 | $\frac{\mathrm{W}}{\mathrm{m}^2\mathrm{K}}$ | [3] |
| $\omega_b$ | Blood perfusion rate | .02 (brain), 4.36e-4 (skull), 4.58e-4 (fat),8.83e-3 (skin) | $\frac{1}{\mathrm{s}}$ | [6] |
| $T_b$ | Blood temperature | 37.0 | ℃ | [5] |
| $\sigma_{brain}$ | Electromagnetic conductivity in the brain tissue layer | .765 | $\frac{\mathrm{S}}{\mathrm{m}}$ | [6] |
| $\sigma_{bone}$ | Electromagnetic conductivity in bone (skull) layer | .34 | $\frac{\mathrm{S}}{\mathrm{m}}$ | [6] |
| $\sigma_{fat}$ | Electromagnetic conductivity in fat layer | .11 | $\frac{\mathrm{S}}{\mathrm{m}}$ | [6] |
| $\sigma_{skin}$ | Electromagnetic conductivity in skin layer | .87 | $\frac{\mathrm{S}}{\mathrm{m}}$ | [6] |

| | | | | |
|---|---|---|---|---|
| $E$ | Electric field intensity from cell phone | 40.3 | $\frac{V}{m}$ | See calculations |
| $\mu_r$ | Relative magnetic permeability | 1 | - | [6] |
| $\varepsilon_r$ | Relative dielectric constant | 45.805 (brain), 20.709 (skull), 11.33 (fat), 41.41 (skin) | - | [6] |
| $E_0$ | Incident plane wave | 40.3 | $\frac{V}{m}$ | See calculations |
| $Z_{in}$ | Input impedance | 75 (3D only) | Ω | [10] |
| $I_1$ | Electric current magnitude | 0.6 | A | [10] |
| $V_1$ | Voltage along edge | 45.5 (3D only) | $\frac{V}{m}$ | [10] |
| $T_b$, $T_i$ | Arterial Blood Temp. | 37.0 | ℃ | [6] |

## B. Calculations

The electric field generated by the cell phone is considered to be conserved, therefore $E = E_0$ (the incident plane wave $E_0$ is equal to the electric field intensity source). The electric field $E$ was calculated by solving Equation 12 for $E$ with a SAR value of 1.25 W/kg for the iPhone 5 (the current most popular model) [11]:

$$SAR = \frac{\sigma_{tissue}}{\rho_{tissue}} |E|^2 \quad \text{[Equation 12]}$$

$$E = \sqrt{SAR \frac{\rho_{skin}}{\sigma_{skin}}} = \sqrt{1.25 \frac{1125\ (\frac{kg}{m^3})}{0.87\ (\frac{S}{m})}} \cong 40.3 \frac{V}{m}$$

## C. Mesh and mesh convergence

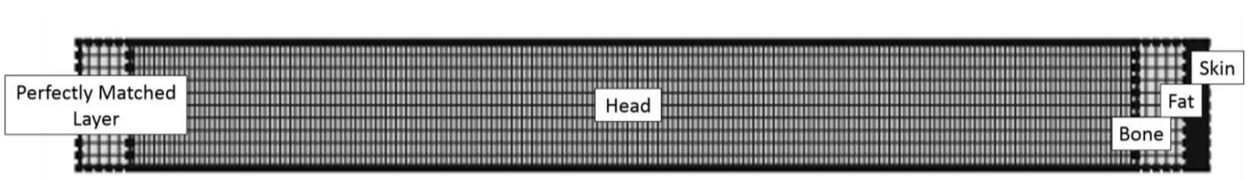

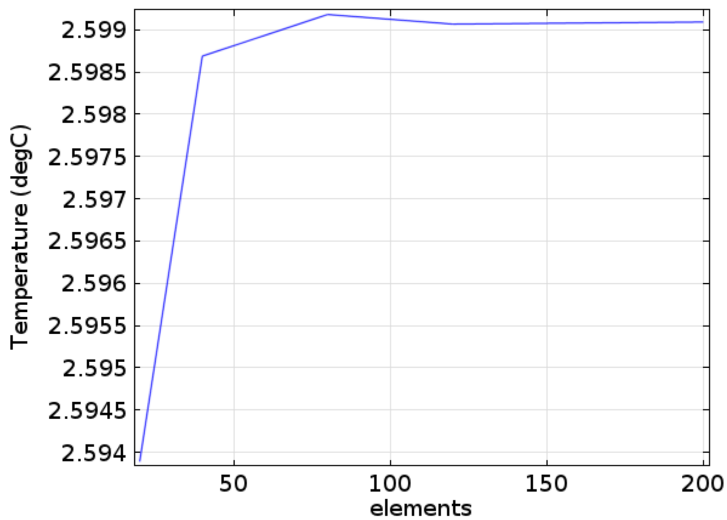


**Figure 9**: Mesh for the model of the head (top) and mesh convergence for brain/skull interface (bottom) for the 2D model. A structured mesh was chosen using 10 elements vertically, 5 elements horizontally beside the brain region, and 120 elements horizontally for the brain region using results from mesh convergence analysis.

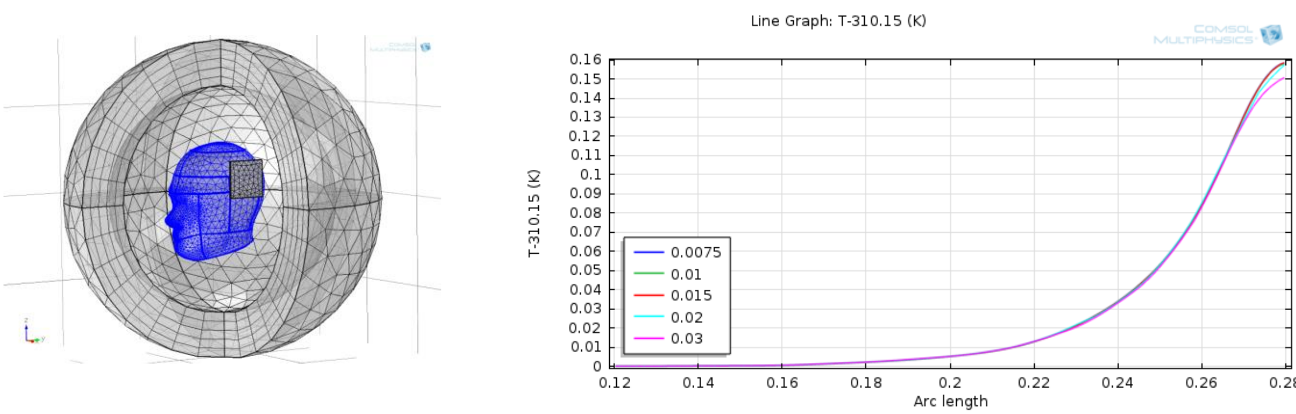


**Figure 10:** Three-dimensional model of the head (left), with a layer of spherical air domain. Free triangular mesh of the head, free tetrahedral mesh of the cell phone domains, and free tetrahedral mesh of the spherical air domain. Mesh convergence of a line through the head (right). Temperature is plotted versus distance along the head (cross sectional line through the head). Temperature stops changing when a maximum triangular mesh size of 0.015 is used.

## XI. APPENDIX B: REFERENCES

[1] Environmental Working Group. (2009). *Cell Phone Radiation: Science Review on Cancer Risks and Children's Health* [Online]. Available: http://www.ewg.org/cellphoneradiation/executivesummary
[2] National Cancer Institute. (2013). *Cell phones and cancer risk* [Online]. Available: http://www.cancer.gov/cancertopics/factsheet/Risk/cellphones
[3] engineeringtoolbox.com. (2014). *Convective Heat Transfer* [Online]. Available: http://www.engineeringtoolbox.com/convective-heat-transfer-d_430.html
[4] J. Dlouhý, "The thermal distribution and the SAR calculation of RF signal inside the human head," Ph.D. dissertation, Dept. Elect. Eng. and Comm., Brno Univ. of Tech., Brno, Czech Republic, 2008.
[5] P. Wainwright, "Thermal effects of radiation from cellular telephones," *Phys Med Biol*, vol. 45, no. 8, pp. 2363-72, 2000.
[6] T. Wessapan and P. Rattanadecho, "Numerical analysis of specific absorption rate and heat transfer in human head subjected to mobile phone radiation: Effects of user age and radiated power," *J. Heat Transfer*, vol. 134, no. 12, pp. 121101-121110, 2012.
[7] J. Wiart *et al*., "Analysis of RF exposure in the head tissues of children and adults," *Phys Med Biol*, vol. 53, no. 13, pp. 3681-95, 2008.
[8] S. M. J. Mortazavi *et al.*, "Human short-term exposure to electromagnetic fields emitted by mobile phones decreases computer-assisted visual reaction time, " *Acta neurologica Belgica*, vol. 112, no. 2, pp. 171-175, 2012.
[9] S.A.R. Mortazavi *et al*., "Exposure to mobile phone radiation opens new horizons in Alzheimer's Disease treatment," *Journal of Biomedical Physics and Engineering*, vol. 3, no. 3, pp. 109-112, 2013.
[10] COMSOL. (2013). *Absorbed Radiation (SAR) in the Human Brain* [Online]. Available: http://www.comsol.com/model/absorbed-radiation-sar-in-the-human-brain-2190
[11] Sarvalues.com, Inc. (2014). *iPhones* [Online]. Available: http://sarvalues.com/iphones/